Supporting Information

Engineering excited state absorption based nanothermometry for temperature sensing and imaging

K. Trejgis, A. Bednarkiewicz*, L. Marciniak*
Institute of Low Temperature and Structure Research, Polish Academy of Sciences, Okólna 2, 50-422 Wroclaw, Poland

* corresponding author: l.marciniak@intibs.pl
a.bednarkiewicz@intibs.pl

KEYWORDS tetraphosphates, excited state absorption, resonant and non-resonant excitation, luminescence thermometry

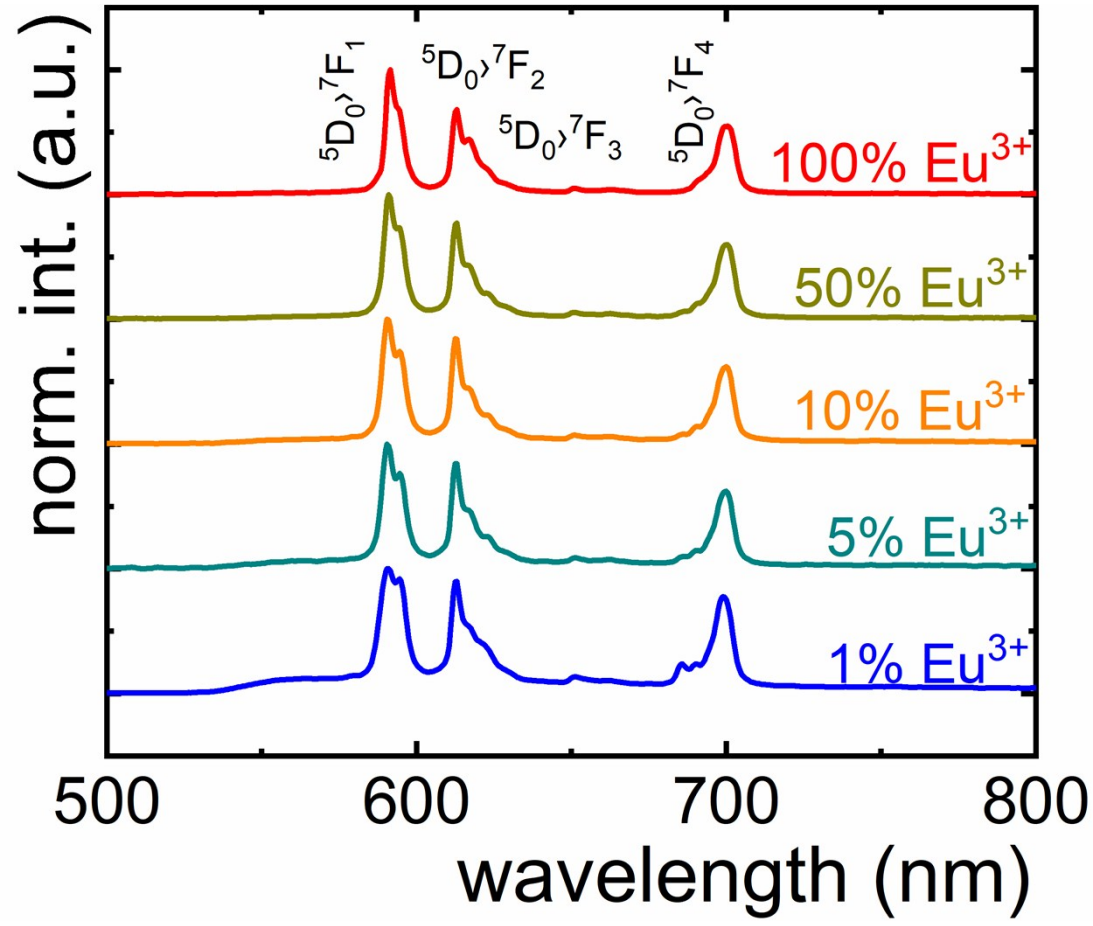

Figure S1. Normalized Stokes emission spectra of $LiLaP_4O_{12}$: Eu^{3+} with different Eu^{3+} ions concentration.

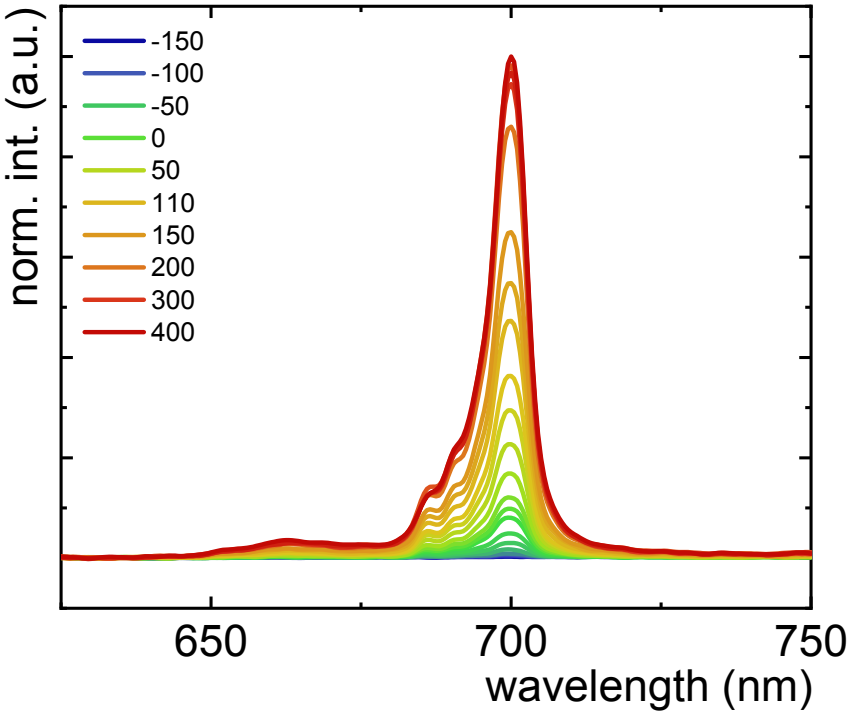

Figure S2. Thermal evolution of $LiLaP_4O_{12}$: 50%Eu nanocrystals emission band at 695 nm ($^5D_0 \rightarrow {}^7F_4$ transition) upon 620 nm excitation.

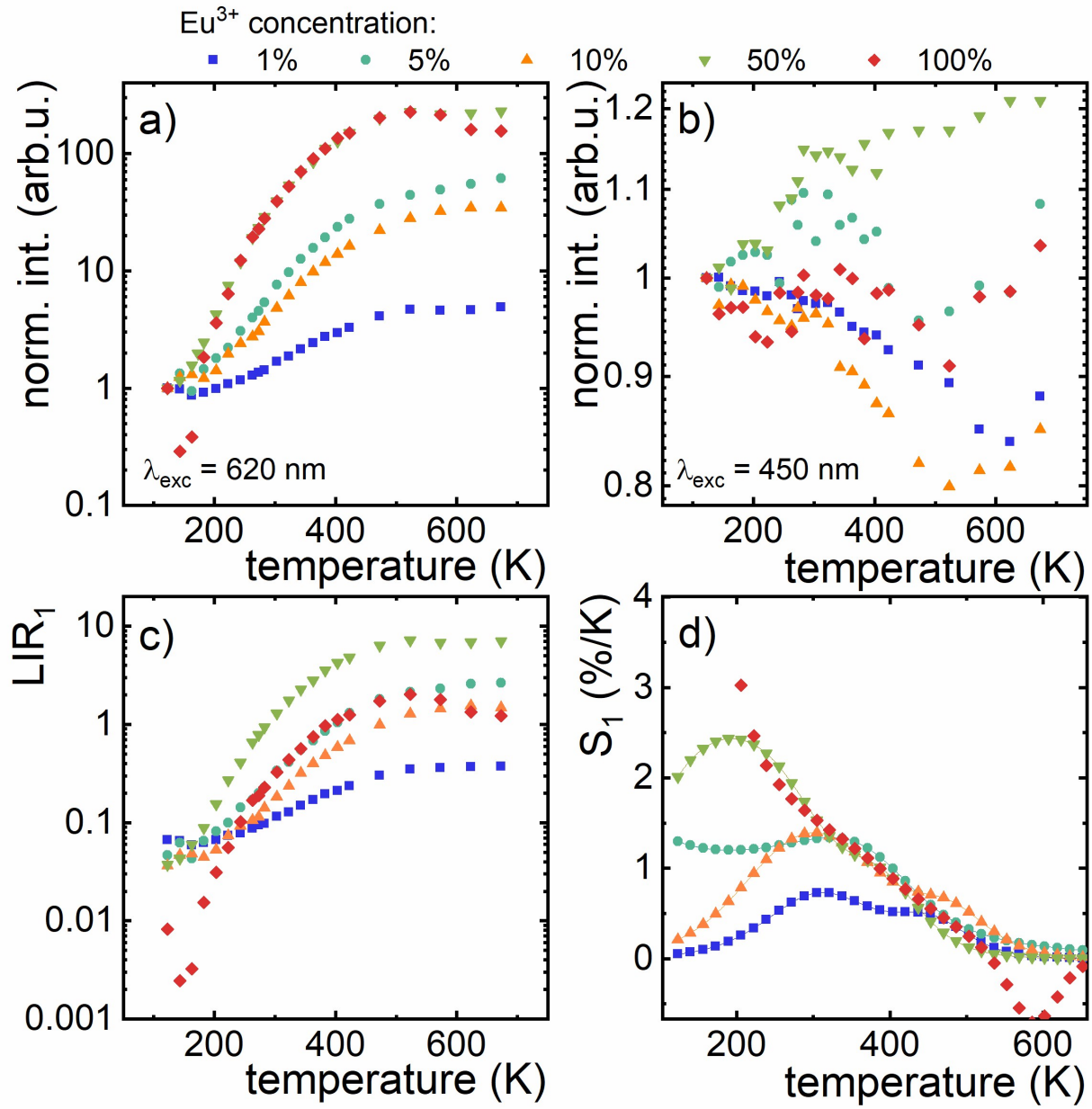

Figure S3. The influence of Eu^{3+} ions concentration on thermal evolution of integral emission intensity of $LiLaP_4O_{12}$: Eu^{3+} nanocrystals upon excitation wavelength of 620nm (a) and 450 nm (b) (the intensities were normalized to the value at the lowest measured temperature for respective Eu^{3+} concentrations); thermal evolution of LIR_1 (c) and S_1 (d) of $LiLaP_4O_{12}$: Eu^{3+} with different Eu^{3+} ions concentration.

To demonstrate the feasibility of the proposed methods for temperature imaging, the proof-of-the-concept imaging studies have been performed on a sample as is schematically presented in S4. It is composed of Peltier element with radiator (to keep the stage at constant temperature, teflon chamber for power sample. Thought this chamber, a tungstate wire was placed and power supplied with a laboratory power supply with electrical currents from 0 to 7A.

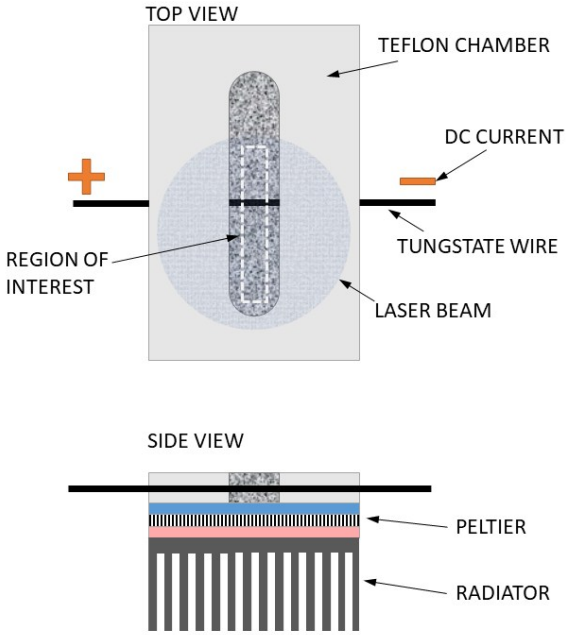

Fig.S4. Schematic outlook of the sample chamber and experimental setup.

The sample was observed using Canon EAS 400D digital camera equipped with 50 mm macro lens and a emission filter to remove excitation wavelength. Static images were recorded for the two excitation lines with constant acquisition times (t_{GSA} = 1 s, t_{ESA}= 8 s) and for rising electrical current (0..7A) supplying the tungsten wire (Fig.S8). Then the images were processed in Matlab, as described in main article. Next, the wire images have been recorded and the acquired images at GSA and ESA photoexcitation have been extracted, i.e. the R frame, out of RGB color image (Fig.S7) for rising current supply (from 0A to 7A). Only region of interest on these images (Fig.S7) was used for further analysis (Fig.S9 and S10).

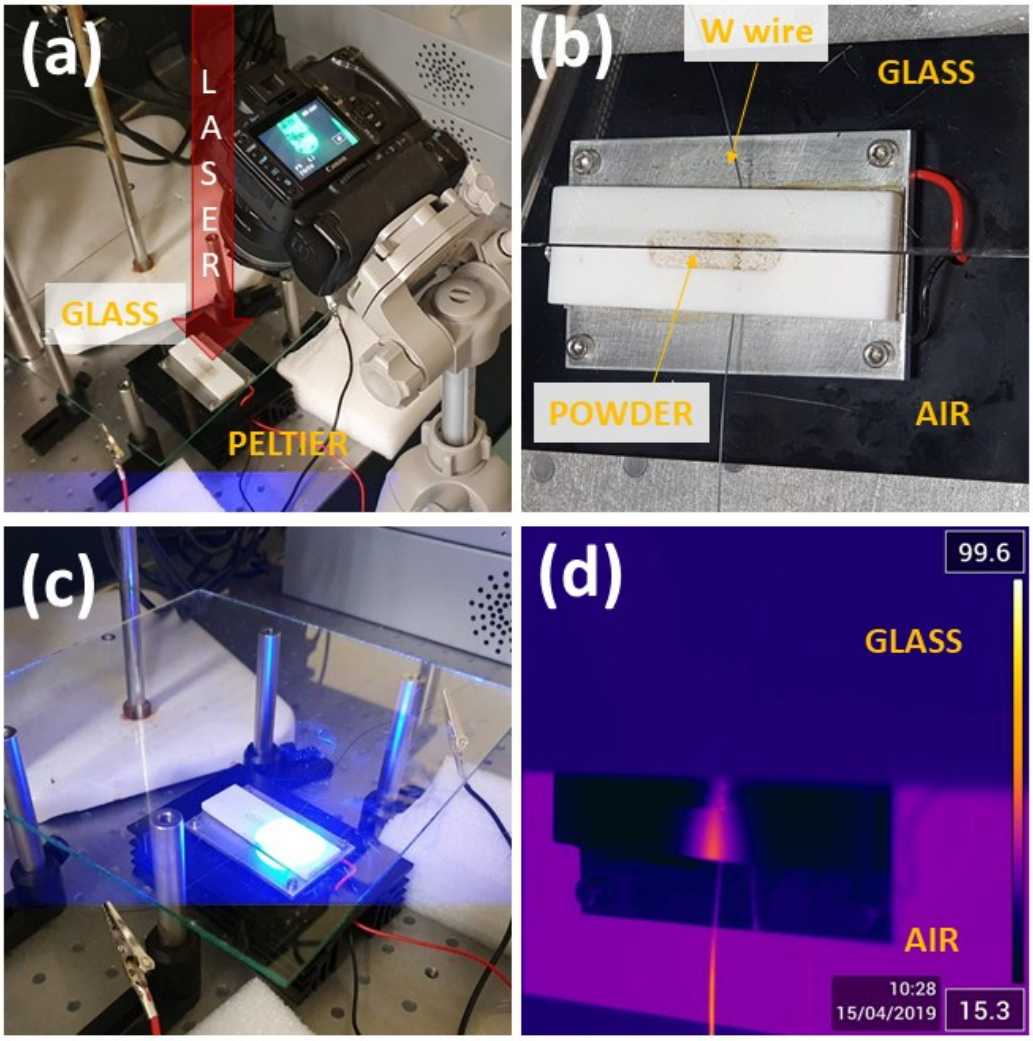

Fig.S5 Experimental setup. experimental setup with a digital camera (a) the sample chamber (b), through the glass temperature monitoring with the phosphor technology (c), the evidence that the bolometric camera cannot record temperature throughout the glass (d).

Using “normal” ratiometric single point detection is relatively simple – single excitation wavelength excites luminescence, which is collected through dichroic filter using CCD spectrophotometer. Based on the obtained spectra, LIR is determined and based on calibration curve, temperature is derived. The ESA based idea is more complex in this respect because 2 excitation wavelengths are needed, but the emission collection path is identical as in the case of “normal” ratiometric single point detection.

The real advantage of our approach is however achieved in imaging mode. The “normal” ratiometric images require either (i) hyper spectral camera - sensitive camera with liquid crystal tunable filter (costly), (ii) fixed dichroic filter with 2 cameras (one needs to identical cameras, so the cost is x2), which after synchronization gives simultaneous acquisition of both spectral

regions or (iii) using mechanic switching between 2 different filters with one camera (images are collected in sequence), which is relatively slow if you need to switch the filters with a filter wheel. These methods have more issues if the emission of thermometer, i.e. the emission bands used for LIR spectral overlap, since some spectral bleeding may occur or the sample may affect the emission ratio in different way depending on the wavelength. Our approach simplified the things, because single camera is required and 2 light sources (e.g. laser diodes), which can be switched by electronic trigger – this is much faster and cheaper solution.

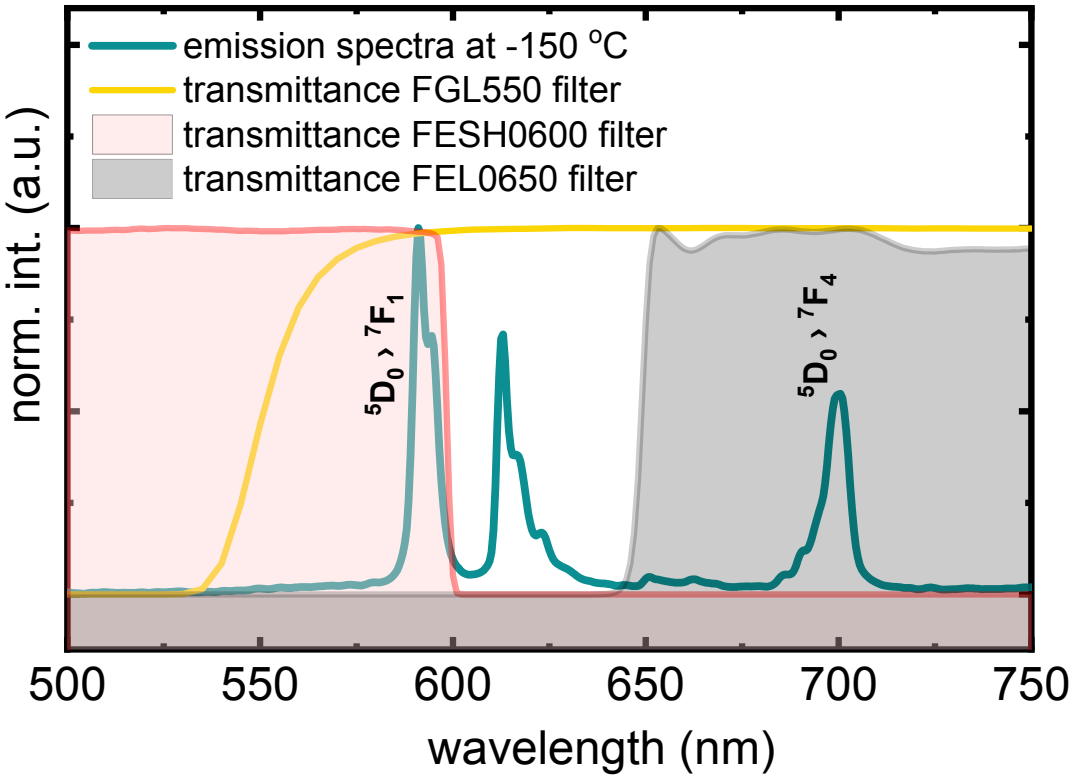

Fig.S6. Spectral features of the filters used to transmit the Eu^{3+} emission under resonant and non-resonant photoexcitation.

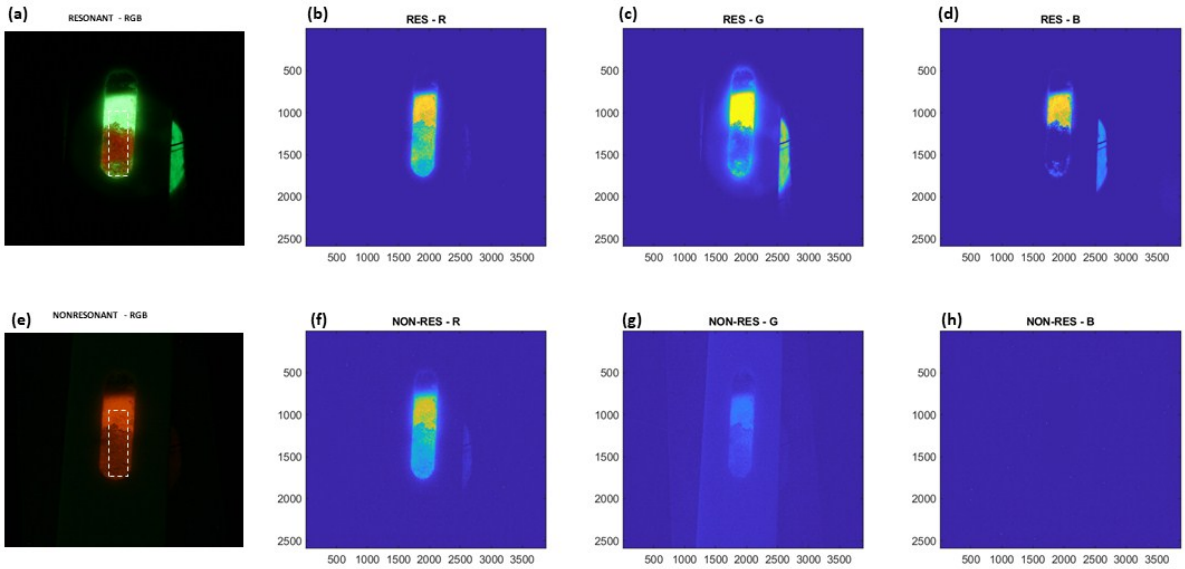

Fig.S7. Exemplary luminescence images obtained with a RGB camera and macro lens. First column (a) and (e) – actual RGB images; second (b) and (f) , third (c) and (g) and fourth (d) and (h) columns correspond to R,G and B colour channels of color RGB image, for resonant (first row, λ_{exc}=450 nm, λ_{emi}=690 nm) and non-resonant (second row, λ_{exc}=620 nm, λ_{emi}=690 nm) excitation scheme, respectively. For further analysis, region of interest (marked by white broken line rectangle on (e)) is taken into account.

The thermal images acquired with conventional thermographic camera enabled to relate the current with the temperature of the wire (Fig.S8).

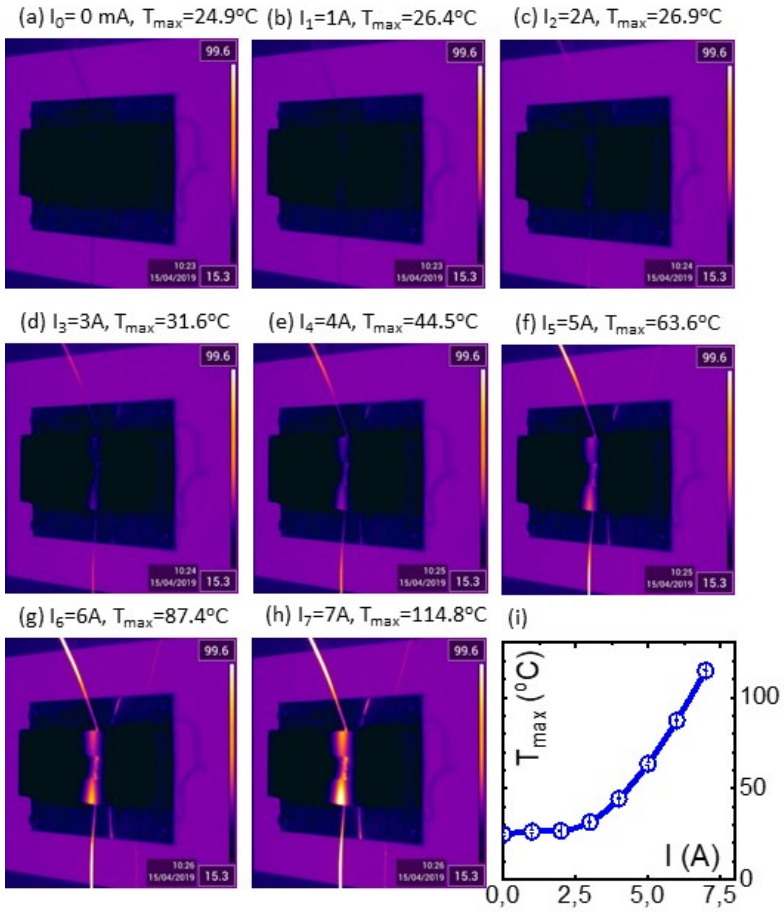

Fig.S8. The calibration of luminescent nanothermometers using temperature of a tungstate wire at rising (0..7A) current supply.

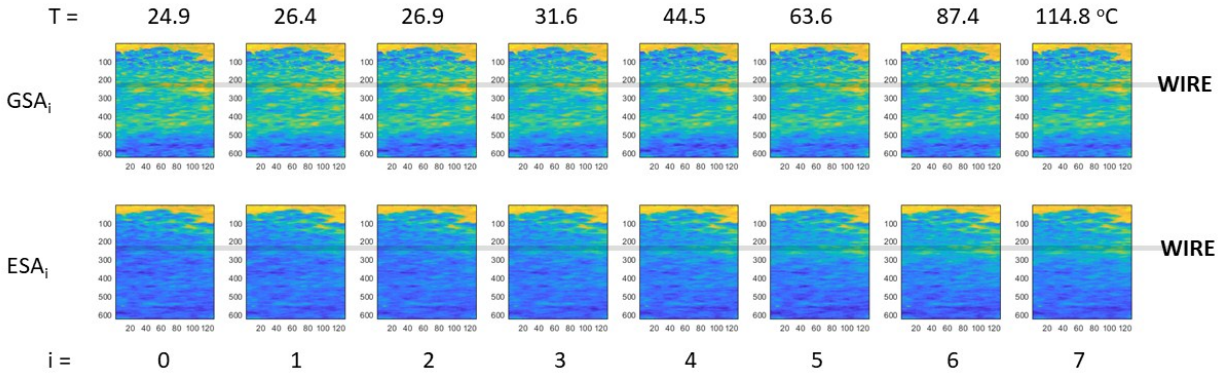

Fig.S9. R image extracted out of colour RGB images under GSA_i (top row) and ESA_i (bottom row) at rising current (i=0..7A) supplying the tungsten wire (position of the wire is marked on the images).

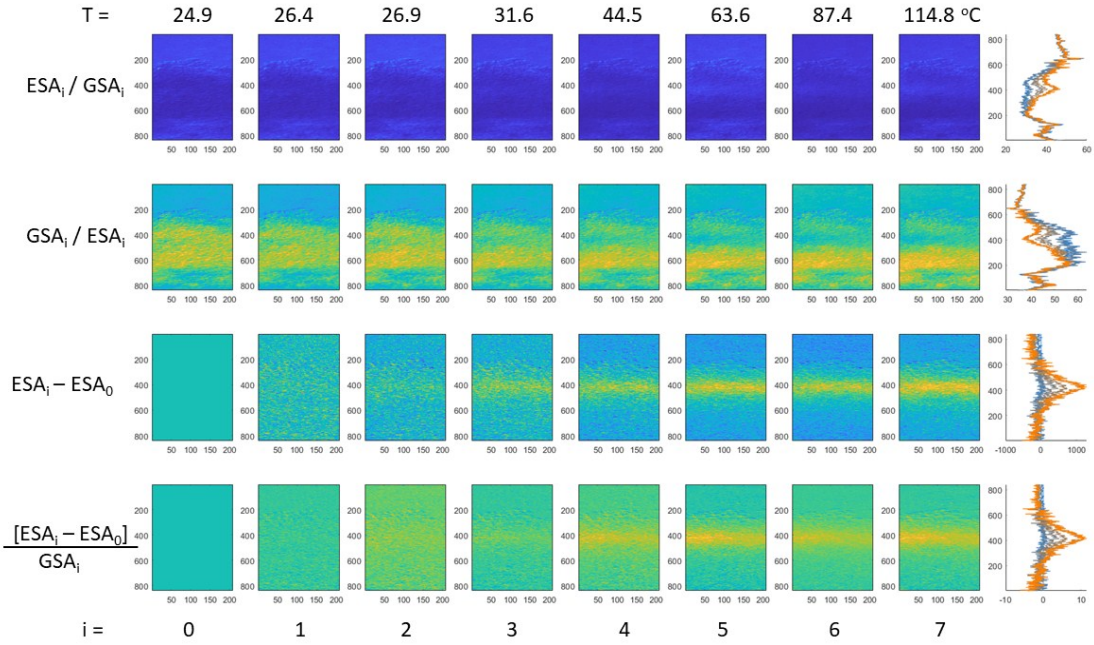

Fig.S10. An example analysis performed on the images from Fig.S8. The mathematical formula used to get the transformed images are presented on the most left column. Images obtained with increasing current, and thus increasing temperature for each mathematical formula presented in the middle of the Fig 10 (columns 2-9). The outcome cross section of the subsequent images are presented in the most right column.